

Bulk electronic structure of Ce compounds studied by x-ray photoemission and x-ray absorption spectroscopies

P. Vavassori and L. Duò

Istituto Nazionale di Fisica della Materia-Dipartimento di Fisica, Politecnico di Milano, piazza L. da Vinci 32, I-20133 Milano, Italy

G. Chiaia,* M. Qvarford, and I. Lindau

Department of Synchrotron Radiation Research, Lund University Sölvegatan 14, S-22362 Lund, Sweden

(Received 19 July 1995)

The results of a systematic x-ray absorption spectroscopy (XAS) investigation across the Ce $M_{4,5}$ and $N_{4,5}$ thresholds for CeCo₂, CeRh₂, CeRh₃, and Ce₇Rh₃ are reported. The data have been analyzed by employing a simplified version of the Anderson single-impurity model in the infinitely narrow bandwidth approximation for the extended states. The model has been applied to the bulk Ce 3d XPS spectra of these compounds. The bulk values of the Ce 4f-occupation number n_f and of the 4f extended states interaction strength Δ obtained have been checked by applying the model to the bulk sensitive Ce $M_{4,5}$ XAS line shapes. The possible influence of a configuration dependence of the hybridization strength in the n_f and Δ determination has been discussed. This joint analysis allowed us to obtain an accurate estimation of n_f . The Ce $N_{4,5}$ XAS line shapes are in agreement with the deduced trend of the 4f electrons interaction strength with the conduction electrons in the bulk.

I. INTRODUCTION

The peculiar behavior of the 4f electrons of Ce and its compounds has been the subject of many experimental and theoretical studies.¹ In particular, there have been extensive efforts to estimate the Ce 4f-occupation number in the ground state, which is closely related to the Ce valence. Among the theories proposed to relate the ground-state properties to the observed spectroscopic results, the Anderson single-impurity model in the formalism of Gunnarsson and Schönhammer (GS) (Ref. 2) has often been used successfully. The spectral line shape for the various spectroscopies calculated within this framework depends upon a number of parameters, namely the ground-state Ce 4f-occupation number n_f , the f -level binding energy, the Coulomb correlation energy of the 4f electrons, the hybridization energy Δ between f and the conduction states and, in presence of a core hole, the Coulomb interaction energy between a 4f electron and the core hole. The comparison between the calculated and measured spectra should allow one to obtain the set of parameters for the system under investigation. In practice, due to the great number of parameters involved and to the ambiguity in their determination, it is desirable to have more than one single experimental guideline. In this work we concentrate on the estimation of the 4f occupation number n_f and of the 4f electrons interaction strength with the other conduction electrons for a set of Ce intermetallic compounds. To this aim Ce 3d x-ray photoemission spectroscopy (XPS) is often used, since from the spectral shape analysis the n_f and Δ values can be assessed with good accuracy.³ Recently the study of surface effects on the correlated electronic structure of these compounds has attracted considerable attention.^{4,5} Surface effects are important in terms of both 4f surface

binding-energy shift⁶ and 4f configuration change of the Ce atoms in the surface region, due to the reduction of the coordination. The last effect is particularly evident for strongly hybridized systems which show a much lower hybridization degree at the surface as compared to the bulk.^{4,5} Due to the surface sensitivity of the XPS technique, for the Ce 3d XPS results analysis, it is essential to disentangle the bulk contribution from the surface one. The decomposition of the XPS spectrum into bulk and surface components is usually carried out by comparing spectra taken at different photon energies, i.e., with a different surface sensitivity resulting from the escape depth vs electron kinetic-energy variation. Owing to the large number of spectral components (six for the bulk and six for the surface),⁴ and to the rather small measured surface effect, the decomposition is usually affected by large uncertainties. X-ray absorption spectroscopy (XAS) across the Ce 3d threshold does not have the surface sensitivity of XPS, and the analysis of its spectral shape, without any decomposition into bulk and surface components, can be exploited to assess n_f and Δ in the bulk.^{7,8} Thus an XAS investigation provides an important check on the conclusions derived from the XPS studies.

In principle, however, the estimation of n_f from XPS and XAS could yield slightly different values due to the different 4f configuration dependence of Δ ⁹ in the two spectroscopies. We report in detail the results of a systematic XAS investigation across the Ce $M_{4,5}$ and $N_{4,5}$ thresholds for CeCo₂, CeRh₂, CeRh₃, and Ce₇Rh₃. We have selected the Ce-Rh phase diagram, which received great attention in the last years, since it gives rise to compounds spanning from the poorly hybridized to the strongly hybridized ones.^{4,10} On the other hand, the comparison between isostructural CeCo₂ and CeRh₂ allows

one to highlight the effects of the variation of the Ce partner. For the analysis we employed a simplified version of the GS model in the infinitely narrow bandwidth approximation for the extended states,¹¹ which fully accounts for the dependence of the experimental results upon the single-impurity model parameters, within a very simple framework. The model has been applied to the bulk component of measured Ce 3*d* XPS spectra of these compounds,¹² and the values of n_f and Δ so obtained have been checked by applying the model to the Ce $M_{4,5}$ XAS line shapes. This joint analysis indicated that both spectroscopies can be well described by the same set of parameters, and allowed us to obtain an accurate estimation of n_f and of the trend of the 4*f* conduction electrons' interaction strength in the bulk. Moreover we observed that the Ce $N_{4,5}$ XAS line shapes are in agreement with results deduced from Ce $M_{4,5}$ XAS and Ce 3*d* XPS.

II. EXPERIMENT

The samples are polycrystals prepared by induction melting from stoichiometric amounts of the compounds in Ta crucibles after Ar purging. They were annealed at 800–900 °C for several days in order to obtain homogeneous polycrystals checked then by x-ray diffraction and microprobe analysis. The crystal structure types are that of MgCu₂ for CeCo₂ and CeRh₂, that of Cu₃Au for CeRh₃, and that of Th₇Fe₃ for Ce₇Rh₃. The XAS spectra were obtained by recording the partial electron-yield signal with an electron kinetic-energy window of 0–10 eV. The measurements have been carried out at the soft-x-ray beam line 22 at the MAX synchrotron radiation laboratory in Lund¹³ in normal-emission geometry. Overall energy resolutions of about 0.1 and 0.7 eV were achieved at the Ce 4*d* ($h\nu \sim 120$ eV) and Ce 3*d* ($h\nu \sim 880$ eV) thresholds, respectively. The samples were cleaned in vacuum (base pressure 7×10^{-11} mbar) by scraping with a diamond file immediately before the measurements. The samples were kept at ~ 100 K, during the scraping and the measurements, in order to avoid surface contamination due to segregation of impurities from the bulk. The sample cleanliness has been checked via the O 1*s*, C 1*s*, and O 2*p* XPS signals. The surface segregation could also induce changes of the surface composition. Thus the surface stoichiometries have been accurately checked by use of core-level peak intensities of x-ray photoemission spectra, and were found to be in excellent agreement with the bulk stoichiometries.¹⁴

III. RESULTS AND DISCUSSION

A. $M_{4,5}$ XAS spectra

The XAS spectra at the Ce $M_{4,5}$ threshold of the studied compounds are shown in Fig. 1 along with that of γ -Ce.⁷ The spectra exhibit two main peaks which are known to be due to the $3d_{3/2}$ and $3d_{5/2}$ multiplet structures of the $3d^9 4f^2$ final state.¹⁵ The spectra of CeCo₂, CeRh₂, and CeRh₃ show additional peaks at about 5-eV higher photon energies, labeled by *A* and *B* in Fig. 1. The XAS spectra line shape of Ce₇Rh₃ is quite similar to

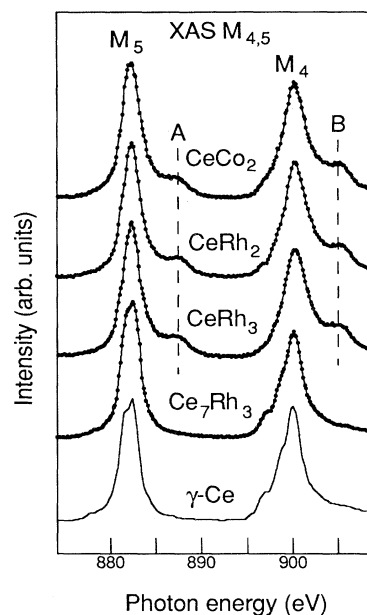


FIG. 1. $M_{4,5}$ spectra of the Ce compounds investigated and of γ -Ce (Ref. 7). The labels *A* and *B* indicate the features related to the $3d^9 4f^1$ final states.

that of γ -Ce, where only the main peaks with a clearly outlined $3d^9 4f^2$ final state multiplet structure is observable. Features *A* and *B* in the CeCo₂, CeRh₂, and CeRh₃ spectra are interpreted as originating from $3d^9 4f^1$ final states.^{7,8} The energy separation (~ 5 eV) of these features from the main peaks is essentially driven by the Coulomb interaction between the 3*d* core hole and the 4*f* subshell, and by the Coulomb repulsion between the 4*f* electrons. This separation is observable in the Ce 3*d* XPS experiments as well, where the $3d^9 4f^1$ and $3d^9 4f^2$ final states are also present.¹¹ Their growth is further accompanied by a shape change of the main peak arising from a washing out of the multiplet structure of the $3d^9 4f^2$ final state. These spectral shape modifications are related to the decrease of the *f* counts and to the increase of the hybridization of the *f* levels with the other conduction states.^{7,8} More precisely, the weight of the features with respect to the main peaks has been found to be related to the weight of the $4f^0$ configuration in the ground state in a quite straightforward way.^{7,8} The growth and intensity of shoulders *A* and *B* in the CeCo₂, CeRh₂, and CeRh₃ spectra indicate a stronger interaction of the 4*f* electrons with the conduction states with respect to CeRh₃ and γ -Ce; on the other hand, the latter (Ce₇Rh₃ and γ -Ce) show a very similar degree of 4*f* conduction state hybridization.¹⁰ These results are consistent with those coming out from the Ce 3*d* XPS (Ref. 12) and resonant photoemission spectroscopy experiments across the 3*d*-4*f* and 4*d*-4*f* thresholds.¹⁶

For a more quantitative analysis of the XAS data of the most hybridized compounds (CeCo₂, CeRh₂, and CeRh₃), we employed a simplified version of the Gunnarsson and Schönhammer (GS) model proposed by Imer and Wuilloud.¹¹ In this model the energy splittings and

relative intensities of the final-state features of the XAS spectra are calculated as a function of the parameters ϵ_f , U_{ff} , U_{fc} , and Δ . Here ϵ_f stands for the energy of the unhybridized $4f$ level relative to the Fermi level E_F , U_{ff} for the Coulomb repulsion between $4f$ electrons at the same site, U_{fc} for the Coulomb attraction energy between a $4f$ electron and a Ce $3d$ core hole, and Δ is an effective parameter accounting for the hybridization energy between $4f$ and the conduction states. The assumption of an infinitely narrow band neglects the continuous distribution of the spectral density, which results from the energy dispersion of the band states. Therefore the spectral functions obtained are distributed on infinitely narrow lines. Despite this limitation the model takes fully into account the fundamental mechanisms of hybridization, and allows one to effectively address the influence of the single-impurity model parameters on the experimental spectra. A set of parameters for each compound was determined by fitting the model to the XPS spectra. As pointed out in Sec. I, an important effect which must be taken into account is the lowering of the $4f$ hybridization strength at the surface, as compared to the bulk which is particularly crucial in the strongly hybridized compounds.^{4,5} For this reason, due to the non-negligible surface sensitivity of our XPS measurements (electron kinetic energies of ~ 360 and ~ 580 eV for Mg- ka and Al- ka lines, respectively), a previous separation of the spectra contribution into the surface and bulk emissions has been carried out. A detailed description of the decomposition procedure is reported in Ref. 12, and the summary of the bulk spectral weights is displayed in Fig. 2. Aiming to compare the XPS with the bulk-sensitive $N_{4,5}$ XAS results, for each compound we selected the set of parameters which better accounts for the intensity and the energy separation of the $3d$ XPS bulk components. The values of ϵ_f have been chosen exploiting the results of the resonant photoemission spectroscopy study in which the surface and bulk spectral contributions to the valence spectra have been separated.¹⁶ The knowledge of ϵ_f in the bulk ($\epsilon_f \cong -1.2$ eV for CeCo₂ and CeRh₃, $\epsilon_f \cong -1.0$ eV for CeRh₂) is essential in order to fix the correct Δ parameter which accounts for the XPS bulk line shape. In fact, somewhat larger values of ϵ_f are expected in the

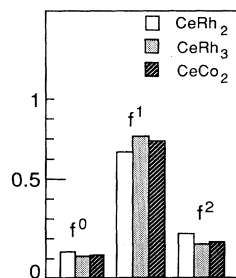


FIG. 2. Summary of the XPS spectral weights of the f^0 , f^1 , and f^2 contributions in CeRh₂, CeRh₃, and CeCo₂ coming from the bulk. The percentage accuracy of the minority components (f^0 and f^2) is better than 15% (for the majority it is much better) (Ref. 12).

surface region due to the $4f$ surface binding-energy shift effect.⁶ For each set of parameters obtained from the XPS analysis, the model returns the correspondent value of the $4f$ -occupation number n_f . The value of Δ and n_f determined by this analysis are displayed in Table I.

By use of the XPS parameters we then calculated the intensity of the XAS features. The comparison between the calculated and measured XAS spectra yields a remarkable agreement, as emerges from the results summarized in Table I, where the ratios (r) between the transition intensity to the $3d^9 4f^1$ final state and the total area of the $M_{4,5}$ peaks from theory and experiment are reported, respectively. In the case of the experimental spectra this ratio has been evaluated by estimating the peak areas. The results reported in Table I indicate that, in the bulk, CeRh₂ is the most hybridized among the investigated compounds, while CeCo₂ and CeRh₃ exhibit a similar degree of $4f$ conduction state interaction, somewhat lower compared to CeRh₂. The n_f value obtained here for CeRh₃ is consistent, within experimental uncertainties, with the bulk one (0.81 ± 0.03) given in Ref. 4, where the Ce $3d$ XPS data have been analyzed by using the same simplified model. The CeRh₃ n_f value we estimated is significantly larger compared with the one (0.78) obtained from the Ce $N_{4,5}$ XAS spectrum prethreshold study reported in Ref. 17, where an ϵ_f value too large (-2.0 eV), considering the bulk sensitivity of the measurements, was assumed in the data analysis. In the case of CeCo₂ the bulk n_f value we estimated is consistent with the one of ~ 0.80 deduced from the valence-band resonant photoemission study reported in Ref. 18, and appreciably larger with respect to that (~ 0.76) obtained in Ref. 19, derived from core electron-energy-loss spectra analysis, which, however, is determined with a lower accuracy ($\pm 10\%$). The present result of a GS description of XAS and XPS spectroscopies with a single set of parameters deserves further discussion in the light of a recent debate on the influence of different configurations of the hybridization strength which here, as usually done, is neglected (i.e., Δ is kept fixed). *Ab initio* calculations of the hopping matrix element V between $4f$ and conduction states have shown that the hybridization strength, which is proportional to V^2 , may vary by a factor ~ 4 for different $4f$ and core electron configurations.⁹ This hybridization strength configuration dependence should modify the configuration mixing in the final state with respect to the initial state, which in turn should result in relative intensities of the spectral structures of different kinds of spectro-

TABLE II. Summary of the results of the analysis of the $M_{4,5}$ spectra of the Ce compounds studied. r is the ratio between the transitions intensity to $3d^9 4f^1$ and $3d^9 4f^2$ final states (see text).

Compound	Δ (eV)	r		n_f
	from XPS	from GS	experiment	(± 0.02)
CeRh ₂	1.05	0.13	0.12–0.13	0.79
CeRh ₃	0.85	0.10	0.10–0.11	0.84
CeCo ₂	0.95	0.11	0.10–0.11	0.83

copies. This problem arose for the description of strongly hybridized systems (e.g., CeRh_3), where a satisfactory description of the results of XPS and bremsstrahlung isochromat spectroscopy in terms of a single set of parameters is not achievable.²⁰ To account for these effects without introducing additional parameters, one should choose an overall (properly averaged on the initial and final state) $\bar{\Delta}$ parameter appropriate for each kind of spectroscopy. In the case of a comparison between XAS and XPS, the situation should be less critical due to the similarity between the two processes, in which the main effect on the hopping matrix elements is the shrinking of the $4f$ wave functions induced by the presence of the $3d$ core hole in the final state of both spectroscopies. However, a somewhat lower value of the overall hybridization strength is expected to occur in XAS with respect to XPS, when considering the effects of expected to occur in XAS with respect to XPS, when considering the effects of the f^0 , f^1 , and f^2 final-state configurations for XPS, and only f^1 and f^2 for the XAS.⁹ It is worth noting that the overall hybridization strength in XPS is expected to be very similar to that occurring in the ground state, and accounting for the thermodynamic properties.⁹ As a consequence of the different hybridization strengths, a lower value of $\bar{\Delta}$ should be required for the experimental XAS spectral shape description with respect to XPS. Regarding the XAS configurations which are relevant in determining the overall hybridization strength, it should be noted that, although the increase in the f count causes a sudden increase of the Coulomb repulsion energy which prevents an occupancy beyond the double in the ground state, the energy gain due to the presence of the $3d$ core hole allows such an occupancy in the final state. In addition, the energy of the $3d^9 4f^3$ final state is expected to be intermediate between those of the $3d^9 4f^1$ and $3d^9 4f^2$ final states, when considering the typical values of U_{ff} (~ 7.0 eV) and U_{fc} (~ 10 eV) used here for all the compounds according to the literature.⁴ Thus the coupling between the f^2 configuration in the initial state and the f^3 one in the final state should be considered. In the present study, configurations up to f^3 , usually neglected, are therefore taken into account in the final state when applying the GS model to the XAS description, considering that transitions toward the $3d^9 4f^3$ final state should produce sizable effects on the measured XAS spectra of strongly hybridized systems,²¹ for which the weight of the f^2 configuration in the initial state is not negligible.²² The presence of the additional f^2 - f^3 coupling channel increases the overall hybridization strength in the XAS spectra, therefore reducing the difference between the two spectroscopies. This explains the good GS description of both XAS and XPS results with the same set of parameters obtained here, furthermore assuring the reliability of the bulk n_f values and hybridization strength trend obtained from the present XAS vs XPS comparison.

B. $N_{4,5}$ XAS spectra

Figure 3 displays the XAS spectra across the Ce $N_{4,5}$ threshold of the studied compounds along with that of γ -

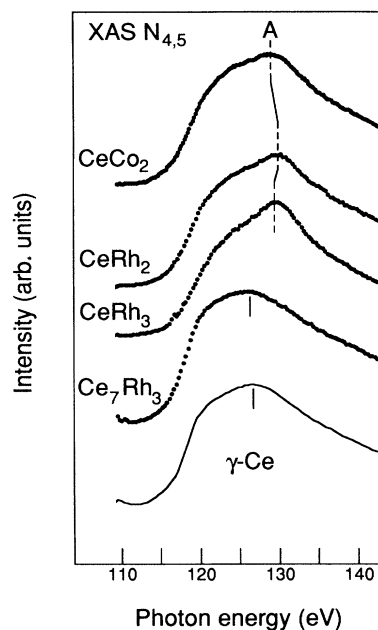


FIG. 3. $N_{4,5}$ spectra of the Ce compounds studied and of γ -Ce from Ref. 24.

Ce.^{23,24} The spectra are characterized by a broad peak corresponding to a $4d^9 4f^{n+1}$ final-state transition. The $4d^9 4f^{n+1}$ multiplet structure extends over more than 20 eV due to the strong exchange interaction caused by the large radial overlap between the $4d$ and $4f$ orbitals. These structures are strongly broadened by autoionization into the underlying continuum,²⁵ and furthermore complicated by the rather small spin-orbit splitting of the $4d$ core hole. For the above-mentioned reasons, at variance with the case of $M_{4,5}$ XAS, the interpretation of the $N_{4,5}$ XAS is still controversial, and only qualitative information about the hybridization strength could be gained from the data analysis. The most striking result is the observation of a feature at ~ 130 eV of photon energy (labeled *A* in Fig. 2) in the $N_{4,5}$ XAS spectra of CeCo_2 , CeRh_2 , and CeRh_3 which is characteristic of α -Ce and of strongly hybridized Ce metallic compounds.^{23,24} This feature is shifted by ~ 5 eV to higher energies relative to the main features observed for γ -Ce and Ce_7Rh_3 indicated in Fig. 3. Looking more closely, the shift of feature *A* is not exactly the same for the three compounds, but is somewhat larger for CeRh_2 with respect to CeCo_2 and CeRh_3 . The magnitude of the shift has been suggested to be related to the increase of the hybridization strength.^{23,24} The present observation seems to confirm this interpretation of the $N_{4,5}$ XAS spectra, since it is consistent with the trend of the hybridization strength as deduced from the $M_{4,5}$ XAS spectral analysis. As a last point it is worth noting that the relative intensity of feature *A* is quite similar for the two phases of Laves, while it is somewhat higher for CeRh_3 , suggesting that the relative intensity of feature *A* should be related to the crystal structure of the compounds in some way. In this connection the $N_{4,5}$ XAS spectral line shapes are

influenced by details of the autoionization process which in turn are expected to be influenced by lattice changes.²⁴ Therefore, even if this effect cannot be quantified at this stage, the lattice modification which characterizes the phase of Laves crystal structures (CeRh₂ and CeCo₂) with respect to the Cu₃Au one (CeRh₃) could have a significant effect on the relative intensity of feature *A* in the spectral line shape.

IV. CONCLUSIONS

In conclusion, we analyzed the results of a systematic XAS investigation across the Ce *M*_{4,5} and *N*_{4,5} thresholds for CeCo₂, CeRh₂, CeRh₃, and Ce₇Rh₃ employing a simplified version of the Gunnarsson and Schönhammer model in the infinitely narrow bandwidth approximation for the extended states. We exploited the bulk component determination of the Ce 3*d* XPS spectra of the compounds, reported in an earlier study, in order to deduce the appropriate set of parameters which better account for line shapes of both bulk Ce 3*d* XPS and Ce *M*_{4,5} XAS spectra. The possible influence of a configuration dependence of the hybridization strength in the GS parameter determination has been discussed.

This joint analysis indicated that both spectroscopies can be well described by the same set of parameters, and allowed us to obtain a reliable estimation of *n_f* and of the hybridization strength trend in the bulk. In addition the qualitative analysis of the Ce *N*_{4,5} XAS line shapes is in agreement with the trend of the 4*f* electron interaction strength with the conduction electrons, as deduced from Ce *M*_{4,5} XAS and Ce 3*d* XPS.

The results reported here indicate that XAS is a useful tool for studying the 4*f* occupancy and 4*f* conduction-electron interaction in Ce systems, particularly suited in investigations in which an extreme bulk sensitivity is required. In particular we have shown that XAS provides an important check on the results coming from XPS studies on Ce intermetallic compounds for which the surface effects on the 4*f* hybridization are relevant.

ACKNOWLEDGMENTS

We would like to thank L. Braicovich for helpful discussions. This work was partially supported by the Swedish Natural Science Research Council and the Swedish Research Council for Engineering Science.

*Present address: Material Physics, Royal Institute of Technology, S-10044 Stockholm, Sweden.

¹See, e.g., *Handbook on the Physics and Chemistry of Rare Earth*, edited by K. A. Gscheidner, Jr., L. Eyring, and S. Hüfner (Elsevier, Amsterdam, 1987), Vol. 10.

²O. Gunnarsson and K. Schönhammer, *Phys. Rev. B* **28**, 4315 (1983).

³J. C. Fuggle, F. U. Hillebrecht, Z. Zolnierok, R. Lasser, Ch. Freiburg, O. Gunnarsson, and K. Schönhammer, *Phys. Rev. B* **27**, 7330 (1983).

⁴C. Laubschat, E. Weschke, C. Holtz, M. Domke, O. Strebels, and G. Kaindl, *Phys. Rev. Lett.* **65**, 1639 (1990).

⁵L. Z. Liu, J. W. Allen, O. Gunnarsson, N. E. Christensen, and O. K. Andersen, *Phys. Rev. B* **45**, 8934 (1992); E. Weschke, C. Laubschat, T. Simmons, M. Domke, O. Strebels, and G. Kaindl, *ibid.* **44**, 8304 (1991).

⁶See, e.g., B. Johansson and N. Mårtensson, in *Handbook on the Physics and Chemistry of Rare Earth* (Ref. 1), Vol. 10, p. 361.

⁷J. C. Fuggle, F. U. Hillebrecht, J. -M. Esteve, R. C. Karnatak, O. Gunnarsson, and K. Schönhammer, *Phys. Rev. B* **27**, 4637 (1983).

⁸G. Kaindl, G. Kalkowski, W. D. Brewer, B. Persheid, and F. Holtzberg, *J. Appl. Phys.* **55**, 1910 (1984).

⁹O. Gunnarsson and O. Jepsen, *Phys. Rev. B* **38**, 3568 (1988).

¹⁰P. Vavassori, L. Duò, L. Braicovich, and G. L. Olcese, *Phys. Rev. B* **50**, 9561 (1994).

¹¹J. -M. Imer and E. Wuilloud, *Z. Phys. B* **66**, 153 (1987).

¹²L. Braicovich, L. Duò, P. Vavassori, and G. L. Olcese, *Surf. Sci.* **331-333**, 782 (1995).

¹³J. N. Andersen, O. Björneholm, A. Sandell, R. Nyholm, J. Forsell, L. Thånell, A. Nilsson, and N. Mårtensson, *Synch. Radiat. News* **4**, 15 (1991).

¹⁴The accuracy of our x-ray analysis was greatly improved

thanks to the possibility of comparing samples having the same components but different stoichiometries. This allowed us to avoid any assumption on the variation of the instrumental efficiency vs photoelectron kinetic energy, on the photoionization cross section and on the electron escape depths.

¹⁵C. Bonnelle, R. C. Karnatak, and J. Sugar, *Phys. Rev. A* **9**, 1920 (1974).

¹⁶G. Chiaia, P. Vavassori, L. Duò, L. Braicovich, M. Qvarford, and I. Lindau, *Surf. Sci.* **331-333**, 1229 (1995).

¹⁷T. Jo and A. Kotani, *Phys. Rev. B* **38**, 830 (1988).

¹⁸J. -S. Kang, J. H. Hong, J. I. Jeong, S. D. Choi, C. J. Yang, Y. P. Lee, C. G. Olson, B. I. Min, and J. W. Allen, *Phys. Rev. B* **46**, 15 689 (1992).

¹⁹G. Strasser, F. U. Hillebrecht, and F. P. Netzer, *J. Phys. F* **13**, L223 (1983).

²⁰D. Malterre, M. Grioni, Y. Baer, L. Braicovich, L. Duò, P. Vavassori, and G. L. Olcese, *Phys. Rev. Lett.* **73**, 2005 (1994); L. Braicovich, L. Duò, P. Vavassori, D. Malterre, M. Grioni, Y. Baer, and G. L. Olcese, *Physica B* **206/207**, 77 (1995); A. Tanaka and T. Jo, *ibid.* **206/207**, 74 (1995).

²¹A. Kotani, T. Jo, and J. C. Parlebas, *Adv. Phys.* **37**, 37 (1988).

²²This is also true for the final state of XPS, but in this case the *f*³ final-state configuration should couple with the *f*³ one in the initial state which does not occur, due to the Coulomb correlation energy.

²³G. Kalkowski, C. Laubschat, W. D. Brewer, E. V. Sampathkumaran, M. Domke, and G. Kaindl, *Phys. Rev. B* **32**, 2717 (1985).

²⁴D. Wieliczka, J. H. Weaver, D. W. Lynch, and C. G. Olson, *Phys. Rev. B* **26**, 7056 (1982).

²⁵J. Connerade and R. C. Karnatak, *J. Phys. F* **11**, 1539 (1981); A. F. Starace, *Phys. Rev. B* **5**, 1773 (1972).